Water and Soil Management and Modeling

Online ISSN: 2783 - 2546

University of Mohaghegh Ardabili

Assessing the impact of global meteorological signals on drought occurrence in Iran

Javad Momeni Damaneh [1]*, Seyed Mohammad Tajbakhsh Fakhrabadi [2], Ehsan Tamassoki [3]

[1] Dept. of Natural Resources Engineering, Faculty of Agriculture and Natural Resources, University of Hormozgan, Bandar Abbas, Iran
[2] Dept. of Watershed Management, Natural Resources Faculty, University of Birjand, Birjand, Iran
[3] Ph.D. in Watershed Management Science and Engineering, University of Hormozgan, Bandar Abbas, Iran

Abstract

This study examined how global climate variations, like the Southern Oscillation Index and North Atlantic Oscillation, affect drought patterns in Iran, causing issues like crop failure, food shortages, and land degradation. To understand these complex relationships, monthly rainfall data from 79 synoptic stations in Iran, collected between 1988 and 2017, were analyzed. The Standardized Precipitation Index was calculated for 3, 5, and 8-month periods to comprehensively assess drought severity and duration across different timescales. The research then examined the correlations between Standardized Precipitation Index (SPI), Southern Oscillation Index (SOI), and North Atlantic Oscillation (NAO), revealing a significant influence of the NAO on Iran's annual precipitation. Variations in pressure systems, particularly the Azores High and the Icelandic Low, were found to impact rainfall patterns nationwide; a 5-month analysis indicated that 66% of the studied stations were affected by these systems. Spatially varying correlations were observed at shorter timescales (5 and 8 months), with some stations like Shahre-Babak showing a positive correlation with NAO, while others like Qazvin exhibited a negative one. Findings indicate that Iran experienced widespread mild to moderate droughts during the study period, excluding the Lake Urmia basin, with minimum SPI values showing a clear trend of change across most of the country. The eastern border region and Qarah-Qom are particularly susceptible to drought, leading to ecological consequences like vegetation changes and increased soil erosion. The period from 1998-2007 was highly drought-prone, while 2008-2017 showed milder conditions. The NAO significantly affected Iran's annual precipitation, impacting 66% of stations. The study highlights the relationship between global climate signals, regional precipitation patterns, and drought, emphasizing its spatial and temporal dynamics. These findings are essential for effective water resource management, targeted drought mitigation, and building resilience to climate variability. Targeted interventions in Eastern Iran, NAO-informed early-warning systems, and strategic water allocation are crucial for drought mitigation.

Keywords: Drought, NAO Signals, Climatic Controlled Index, Standardized Precipitation Index

Article Type: Research Article

*Corresponding Author, E-mail: tajbakhsh.m@birjand.ac.ir
Citation: Momeni Damaneh, J., Tajbakhsh Fakhrabadi, S. M., & Tamassoki, E. (2025). Assessing the impact of global meteorological signals on drought occurrence in Iran. Water and Soil Management and Modelling, 5(Special Issue: Climate Change and Effects on Water and Soil), 62-87.
doi: 10.22098/mmws.2025.17004.1568
Received: 16 March 2025, Received in revised form: 3 May 2025, Accepted: 1 June 2025., Published online: 13 July 2025
Water and Soil Management and Modeling, Year 2025, Vol. 5, Special Issue, pp. 62-87.

Publisher: University of Mohaghegh Ardabili

1. Introduction

Climate change is a pressing global challenge, manifesting in significant fluctuations in climatic phenomena (Vijayavenkataraman et al., 2012). This climatic variability causes substantial economic damage, especially to developing countries with frequent extreme weather events (Mirza, 2003). This variability disrupts global circulation patterns, altering the intensity, frequency, and seasonality of events like El Niño, monsoons, and the Indian Ocean Dipole (Collins et al., 2010; Tokinaga et al., 2012; Cai et al., 2014; Chen et al., 2025). These changes primarily manifest as variations in precipitation, driven by differential heating between land and oceans. Hydrological extremes, particularly floods and droughts, have severe consequences for agriculture and ecosystems (Abhilash et al., 2019). Droughts, characterized by prolonged water scarcity, can lead to significant impacts, including crop failures, food shortages, and mass migration (Schubert et al., 2016; Masih et al., 2014; Akbari et al., 2020). Researchers investigate the influence of global meteorological signals, such as the Southern Oscillation Index (SOI) and the North Atlantic Oscillation (NAO), on regional drought patterns. Analyses of historical data reveal significant correlations between these signals and drought occurrences, particularly in regions like the Iberian Peninsula (Serrano, 2005) and South America (Grimm and Tedeschi, 2009). The El Niño-Southern Oscillation (ENSO) has a notable impact on precipitation events globally. For instance, the positive phase of ENSO is associated with increased precipitation frequency in South America (Grimm and Tedeschi, 2009). In contrast, the negative phase of ENSO and warm phases of other oscillations can lead to increased rainfall in certain regions like Central Asia (Trenberth, 2011). Arid regions, such as Iran, are particularly vulnerable to the impacts of climate change, with increased frequency and severity of droughts (Karandish et al., 2017). These regions often experience both prolonged droughts and intense floods, highlighting the amplified extremes in the hydrological cycle (Madani, 2014). Drought can be categorized into three stages: meteorological, agricultural, and hydrological. Triggered by a rainfall deficit, agricultural droughts are characterized by reduced soil moisture and, hence, a shortage of water supply to vegetation (Dai, 2011; Van Loon, 2015). South Asian floods have been a major point of concern for the past thirty years, exceeding other climatic disasters (Dutta, 2004). Conversely, other areas are impacted by dry conditions during the first months of El Niño years, as well as during the summers and autumns of the following year. ENSO signals reveal a noteworthy impact on precipitation events (Syed et al., 2006), analyzed using correlation analysis, combined analysis, and Singular Value Decomposition (SVD). Recently, such regional correlations have also been explored between Pacific Sea Surface Temperature (SST) and Indian Peninsula rainfall events (Abhilash et al., 2019), showing a weak negative trend that increases with increasing timescale. These impacts demonstrate the sensitivity of headwater stream ecosystems to NAO compounding climate change effects during positive phases, which alter the composition and affect the conservation of ecological function (Durance and Ormerod, 2007). Similar trends have also been experienced along a major African province, which experienced one of the strongest drought events in recorded history in 2016, influenced by the 2015 El Niño (Winkler et al., 2017). Climate change is projected to increase the frequency and severity of multi-year droughts, particularly in North America, Asia, and Africa (Wu et al., 2022). Historical data shows that a significant proportion of multi-year droughts, both past and future, have shorter return periods compared to the last millennium (Wu et al., 2022). SST anomalies, especially those associated with ENSO, play a crucial role in driving meteorological droughts by influencing global precipitation patterns (Schubert et al., 2016). While regions like the Americas and eastern Asia exhibit strong responses to ENSO, others, such as Europe and Africa, show less sensitivity (Schubert et al., 2016). Drought characteristics vary significantly across different regions. Studies show that 47% of major river basins tend drought despite increased precipitation (Zhu et al., 2024). The Drought Exceedance Probability Index (DEPI) reveals that regions with less rainfall variability experience fewer droughts,

while intertropical regions are witnessing longer and more intense droughts (Rodríguez et al., 2022). However, some regions, particularly in northern latitudes, are experiencing increased runoff and shorter drought durations (Vieira & Stadnyk, 2023), highlighting the complex interplay of climatic factors. Recent research has further elucidated the impacts of global meteorological signals on drought occurrence and severity. Studies have demonstrated significant correlations between climate indices like ENSO, NAO, and SST, and regional rainfall patterns and drought characteristics (Karamouz et al., 2004).

Climate models, such as those from the Coupled Model Intercomparison Project (CMIP6), project a significant increase in the spatial extent, duration, and severity of droughts under future warming scenarios (Wu et al., 2022; Zeng et al., 2022; Niu et al., 2025). These models indicate that regions like southern North America, the Mediterranean, and southern Africa are particularly vulnerable to increased drought occurrences. Novel drought indices, such as the Combined Standardized Drought Index (CSDI), have been developed to provide a more comprehensive assessment of drought intensity, duration, and frequency (Nikraftar et al., 2021). These indices show improved sensitivity to teleconnection patterns like ENSO and enhance drought monitoring capabilities. Iran, with 85% of its area in semi-arid and arid climates, faces both prolonged droughts and floods, marking the most enhanced portions of the hydrological cycle. In the southern and northern regions, these events are centered on March and May, respectively. The situation becomes critical when considering that seasonal precipitation amounts in southern Iran have generally increased from autumn to winter and decreased in spring. Conversely, in the northern regions, precipitation has increased during summer and autumn and decreased throughout winter and spring (Nazemosadat et al., 2006). Drought, a complex phenomenon with diverse impacts, is quantified using various indices and influenced by multiple factors, including large-scale climate patterns like El Niño-Southern Oscillation (ENSO) and local atmospheric conditions (Rasmusson et al., 2019; Nieves et al., 2022). ENSO events, characterized by anomalous warming in the equatorial Pacific and shifts in surface pressure (the Southern Oscillation), can exacerbate drought severity in regions like the Orinoco River Basin (Paredes-Trejo et al., 2023). While long-term warming trends contribute to drought conditions, other factors like vegetation health can play a mitigating role (Paredes-Trejo et al., 2023; Nieves et al., 2022).

Drought impacts cascade through different systems, affecting meteorological, hydrological, and agricultural conditions, with increasing magnitude and uncertainty from meteorological to agricultural droughts (Hosseinzadehtalaei et al., 2023). Furthermore, the interdependence of drought duration and severity, often overlooked, significantly amplifies drought risk (Ganguli et al., 2022; Yuce et al., 2025). Remote sensing indices like the Evaporative Stress Index (ESI) offer valuable tools for monitoring drought impacts on vegetation and crop production (Du et al., 2021; Ghazaryan et al., 2020). A Lagrangian approach, tracking drought clusters as they evolve in space and time, reveals that large-scale droughts can propagate over considerable distances and intensify (Herrera-Estrada et al., 2017). This study introduces an integrated approach to examine the combined influence of the Southern Oscillation (SOI) and North Atlantic Oscillation (NAO) on drought patterns in Iran. While previous research has primarily investigated these climate indices in isolation, our simultaneous analysis of both teleconnections represents a novel contribution to the field. Using the Standardized Precipitation Index (SPI) across multiple timescales (3, 5, and 8 months), we systematically quantify interactions between these oscillations and regional drought conditions. This methodology resolves synergistic teleconnection effects, significantly enhancing drought prediction accuracy and informing adaptive water resource management strategies across Iran.

2. Materials and Methods

2.1. Study Area

A great range of elevation from the coast of the Caspian Sea to Damavand peak across Iran includes it in the club of mountainous countries with an average altitude of 1250m above sea

level. The Alborz and Zagros Mountains along north and east Iran play a significant role in one of the hottest deserts of the world, the Lut Desert (Vaghef et al. 2019; Momeny Damaneh et al., 2024). Average annual precipitation of Iran (~251mm) is one-third of the annual precipitation and one-third of the median continental precipitation of Asia over a 1.6 million km^2 area between the Caspian Sea and the Persian Gulf (Balling et al. 2016; Tajbakhsh Fakhrabadi and & Momeny, 2023). The lowest rainfall is observed in the central deserts with less than 25mm, and the highest precipitation, i.e., 1600mm in the Caspian region. Around 1% of the world's population of Iran has just 0.36% fresh water resources and has 250mm annual rainfall in just two-thirds of the total area with uneven annual distribution, i.e., almost half of the precipitation is received during winters (Malekinejad, 2009; Momeny Damaneh et al., 2024).

2.2. Data set

The study includes well-recorded monthly rainfall data of 79 synoptic stations with at least 30 years of statistical records from 1988 to 2017 (Table 1). The SRTM elevation data have been used and processed with the ArcHydro tool to represent six major river basins and the synoptic observation stations of Iran (Figure 1). The alternate precipitation dataset, obtained from the Meteorological Organization of Iran, was employed as a validation and quality-control tool. We conducted a comparative analysis against the primary dataset (79 synoptic stations) using statistical consistency checks, including correlation coefficients at overlapping spatiotemporal points. This cross-verification enhanced anomaly detection robustness, reduced observational uncertainties, and strengthened confidence in SPI-derived drought assessments. An alternate dataset of precipitation is also procured from the Meteorological Organization of Iran; the ENSO and NAO time series were collected through various research centers in Australia, the United States (NOAA), and some European centers (www.esrl.noaa.gov). This alternate dataset is used for a comparative analysis of precipitation.

The data analysis has been done in three major groups according to annual water input frequencies; the first group of 3-months period (March, April and May), the second group of 5-months period (January, February, March, April and May) and the third group of 8-months (October, November, December January, February, March, April and May), are assessed as the water year.

SPI values were derived from monthly rainfall data (1988–2017) for 3-, 5-, and 8-month timescales. The data were stratified into three decades (1988–1997, 1998–2007, 2008–2017) to identify severe drought years and assess SOI/NAO impacts on rainfall fluctuations. Pearson correlation analysis was employed to quantify station-specific relationships between SPI (at each timescale) and SOI/NAO indices using SPSS software. Statistical significance was evaluated at $p < 0.05$ and $p< 0.01$ (in Tables 3 and 4). This method was selected for its sensitivity to linear associations in climate data. Stations exhibiting significant direct/inverse relationships with SOI/NAO were systematically identified. The original data were converted into raster files for spatial analysis (pixel size:100 meters).

Table 1. The characteristics of major river basins of Iran (Tajbakhsh Fakhrabadi and & Momeny, 2023; Momeny Damaneh et al., 2024).

Major basins of Iran	Area (Km^2)	Longitudinal and Latitudinal Extension of Basin	Number of Observation Stations	Altitude (meters)		
				Minimum	Maximum	Average
Caspian Sea basin	1.75×10^5	44.04°E-59.06°E & 34.98°N-39.78°N	18	-271	5594	1374
Persian Gulf and Oman Sea basin	4.24×10^5	44.84°E-63.21°E & 25.06°N-36.92°N	22	-83	4405	971
Urmia Lake basin	5.20×10^4	44.22°E-47.90°E & 35.68°N-38.49°N	6	1175	3730	1735

Central Plateau basin	8.25×10^5	48.12°E-61.42°E & 26.55°N-37.46°N	28	107	4471	1351
Eastern border basin	1.03×10^5	58.59°E-63.33°E & 26.76°N-35.09°N	3	437	3918	1190
Qarah-Qom basin	4.40×10^4	58.20°E-61.28°E & 34.38°N-37.71°N	2	236	3251	1202
Total	1.60×10^6		79			1304

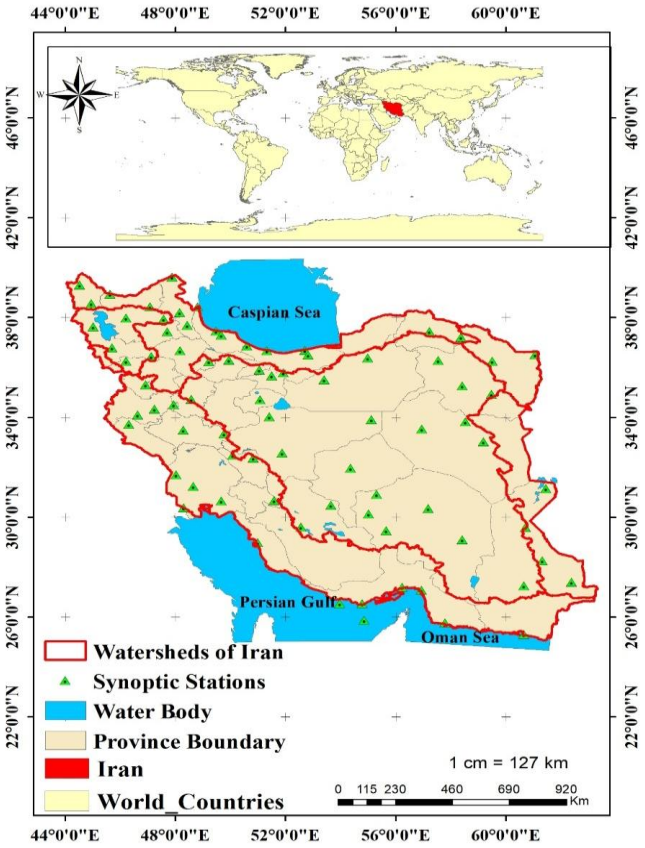

Figure 1. Location of the study area and synoptic stations in Iran

2.3. North Atlantic Oscillation (NAO)

The NAO is a meridional oscillation in the atmosphere, centered near Iceland in the subtropical region (from the Azores to the Iberian Peninsula). The signals of the NAO are used to indicate its phases, gained from the difference in pressure between the Azore's subtropical high pressure and the polar low pressure of Iceland. These signals exhibit two phases: positive and negative. The positive phase is characterized by stronger-than-normal pressure at the Azores high and lower-than-normal pressure at the Icelandic low, resulting in a steep pressure gradient between the two centers. In contrast, the negative phase indicates a weaker subtropical high and a weaker Icelandic low, leading to a reduced pressure gradient (Pasho et al., 2011; Tajbakhsh Fakhrabadi & Momeny, 2023).

2.4. Southern Oscillation Index (SOI)

These signals are intended to quantitatively express the ENSO phenomenon and indicate the gradient of pressure along the east-west Pacific Ocean. In general, it is seasonally and monthly accounted for by the difference in surface water pressure in Tahiti in the central Pacific and Darwin regions of northern Australia, which is consistent with Equation 1. Positive signs indicate the intensity of the Walker stream (La-Niña) and negative signals indicate the weakening of the Walker stream El Niño (Tajbakhsh Fakhrabadi and & Momeny, 2023; Equation 1).

$$P_{diff} = PT_{ahiti} - PD_{arwin} \quad (1)$$

Where, P_{diff} is the water level air pressure difference, P_{Tahiti} is the water level air pressure at Tahiti, and P_{Darwin} is the water level air pressure in the Darwin region.

2.5. Standardized Precipitation Index (SPI)

The Standard Precipitation Index was presented by McKay et al. (1993) to monitor drought spells. They used a categorized system to represent standardized precipitation data. The SPI allows a skilled analyst to quantify droughts or abnormal moisture events on a specified time scale over each region of the Earth where precipitation is recorded (Equations 5,6). Table 2 shows a classification of droughts using the SPI. This index is based on the cumulative probability of precipitation at a station, which, after extracting rainfall data over a statistical period (at least 30 years), forms a time series of total rainfall at the desired scales with a statistical distribution. (McKay et al. 1993; Equation 5,6) set the SPI representation based on the gamma distribution, as follows:

$$g(x) = \frac{1}{\beta^{\alpha}\Gamma(\alpha)} x^{\alpha-1} e^{\frac{x}{\beta}} \quad (2)$$

where, α is the shape characteristic, β is the scale characteristic, x is the amount of precipitation, and Γ is the gamma function obtained from Equations (2,3), as below:

$$\Gamma(a) = \int_0^{\infty} y^{a-1} e^{-y} d \quad (3)$$

Since the Gamma function is not defined for zero values and the rainfall distribution may have zero values, the cumulative probability function, which also includes zero numbers, is defined as the Equation (4):

$$H(x) = q + (1-q)G(x) \quad (4)$$

where, q is the probability of zero in the precipitation values. If M is the number of zeros over a while, Tom (1966) proves that q can be calculated from the division of Mover N (m.n). (X) Use all incomplete gamma function tables to determine the cumulative probability of G. After computing the total cumulative function of H(x), the likelihood transform of the gamma cumulative function is made to the standard normal random variable Z with mean zero and variance of one, which is the probability of the variable being the same as SPI and conversion with the same probability. If the number of stations is high and it is difficult to draw such graphs for all time scales and each month of the year, Z or SPI are easily obtained from the Abramovitz and Estegon approximations, which accumulate probabilities to the standard normal random variable Z converts and is obtained as the Equations 5 and 6, and the values of t as the Equations 7 and 8.

$$Z = SPI = -\left[t - \frac{c_0 + c_1 t + c_2 t^2}{1 + d_1 t + d_2 t^2 + d_a t^a}\right], For\ H(x) < 0.5 \quad (5)$$

$$Z = SPI = +\left[t - \frac{c_0 + c_1 t + c_2 t^2}{1 + d_1 t + d_2 t^2 + d_a t^a}\right], For 0.5 < H(x) < 1 \quad (6)$$

$$t = \sqrt{h\left(\frac{1}{H(x)^2}\right)}, For\ 0 < H(x) < 0.5 \quad (7)$$

$$t = \sqrt{ln\left(\frac{1}{(1-H(x))^2}\right)}, For 0.5 < H(x) < 1 \quad (8)$$

The constant values in the equations are:
$C_0 = 5155117.2$, $C_1 = 802853$, $C_2 = 010328$, $d_1 = 432788.1$, $d_2 = 189269$, $d_3 = 001308$

Conceptually, the SPI represents a sigma score or standard deviation above or below the mean value. Leshi Zand and Tellurie argue that because the classification of McKay and her colleagues was used to determine and monitor drought in the Colorado area, therefore, a specific classification should be selected for each area according to the climate and rainfall regime. According to the location of the region where most of the stations are in arid and semi-arid climates, the following classification is used, which shows precipitation variations in the range -1 to 1 more accurately, and one class was added to the McKay classification (Table 2).

Table 2. Classification of droughts using the SPI index

Class	SPI Values
Severe wet	2
Extreme wet	1.5 to 1.99
The moderate wet	1.49 to 1
Light wet	0.99 to0.5
Normal	0.49 to - 0.49
Mild drought	-0.5 to -0.99
Moderate drought	-1 to -1.49
Extreme drought	-1.5 to -1.99
Severe drought	-2>

3. Results and Discussion

This study analyzes drought patterns across Iran using the Standardized Precipitation Index (SPI) and its correlation with the Southern Oscillation Index (SOI) and the North Atlantic Oscillation (NAO). The research examined three distinct ten-year periods (1988-1997, 1998-2007, and 2007-2017) and six sub-basins (Caspian Sea, Persian Gulf and Sea of Oman, Lake Urmia, Central Plateau, Eastern Border, and Qaraqum), providing a comprehensive overview of drought dynamics. The analysis of minimum SPI values over 3, 5, and 8-month periods reveals a fluctuating drought trend across the country, with the Lake Urmia basin as a notable exception. During the first decade (1988-1997), mild droughts, indicated by the SPI, were prevalent nationwide, with the Central Plateau experiencing the most severe conditions. The subsequent decade (1998-2007) witnessed a shift towards more intense drought, with moderate drought conditions affecting the entire country. Again, the Central Plateau was the hardest hit, while the Lake Urmia basin maintained relatively normal to slightly wet conditions. In the final decade (2007-2017), a lessening of drought severity was observed. Mild droughts were recorded across Iran, with the Central Plateau still experiencing the lowest SPI values, although the Lake Urmia basin continued to experience near-normal to slightly wet conditions. The 5-month SPI during this period, however, indicated moderate drought in the Central Plateau. Overall, the minimum SPI trend suggests a shift from mild drought in the first decade to severe drought affecting the entire country in the second, followed by a decrease in severity and a return to mild drought in the third decade. The study further explores drought through composite indices of SPI and SOI, and SPI and NAO, as well as periodic indices for each of the three decades. For the SPI and SOI composite index, the Caspian Sea sub-basin showed the least severe drought (around -0.4 SPI), while the Qaraqum sub-basin experienced the most severe (around -0.5 to -0.6 SPI) over the three months. When considering the SPI and NAO composite index, the Lake Urmia sub-basin exhibited the least severe drought (close to 0 SPI), while the Eastern Border sub-basin suffered the most severe drought (around -0.1 to -0.2 SPI). Analysis of the periodic indices reveals further regional and temporal variations. During 2008-2017, the Eastern Border sub-basin recorded the most severe drought (around -1 SPI), while the Lake Urmia sub-basin experienced the least severe (around -0.5 to -0.6 SPI). In the 1998-2007 period, the Persian Gulf and Sea of Oman sub-basin was the most drought-stricken (around -1.2 to -1.3 SPI), while the Lake Urmia sub-basin again fared the best (around -0.8 to -0.9 SPI). Finally, for the 1988-1997 period, the Persian Gulf and Sea of Oman sub-basin experienced the most severe drought (around -0.8 to -0.9 SPI), and the Lake Urmia sub-basin the least severe (around -0.6 to -0.7 SPI). In summary, the Eastern Border and Qaraqum sub-basins consistently exhibited the highest levels of drought compared to the other sub-basins. Furthermore, the 1998-2007 and 2008-2017 periods experienced more severe drought conditions than the 1988-1997 period. These findings provide valuable insights for water resource management and the development of effective drought mitigation strategies in different regions of Iran.

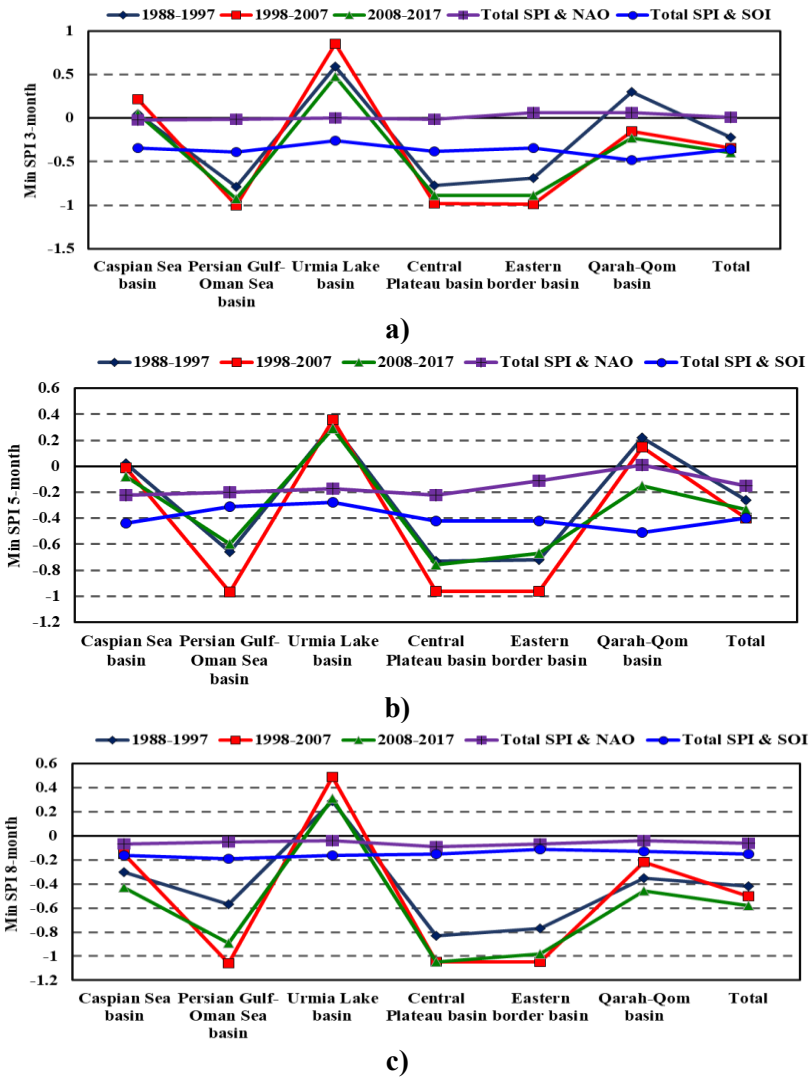

Figure 2. Minimum SPI values during three decades: A- Maximum SPI at a) time scale of 3 months, b) time scale of 5 months, and c) time scale of 8 months

According to Figure 3, the analysis of mean SPI changes reveals a concerning trend of increasing drought, particularly in the eastern border region of Iran. During the second and third decades (1998-2017), this region experienced significant drought conditions. Furthermore, the Central Plateau and the Qarah-Qom region, while classified as "normal," also exhibited signs of mild drought during these periods. The study suggests that a substantial portion of the Central Plateau and Qarah-Qom areas were likely affected by this mild drought, although the classification might not fully reflect the severity on the ground. In contrast, during the earlier period (1988-1997), the Eastern Iranian border basin experienced mild drought in the 3 and 8-month indices. The Central Plateau and Qarah-Qom basins were normal, while the Mazandaran, Lake Urmia, Persian Gulf, and Oman Sea basins experienced slight wetness during the 3, 5, and 8 months. The 5-month index in the eastern border region of Iran shows a normal state over the period 2007-2017. A comparative analysis of SPI in conjunction with SOI and NAO indices reveals distinct regional variations in drought severity. When considering the SPI and SOI composite index over three months, the Caspian Sea sub-basin exhibited the lowest level of drought

(around -0.4), while the Qara Qum sub-basin experienced the highest (around -0.5 to -0.6). Similarly, the SPI and NAO composite index over three months showed the Lake Urmia sub-basin with the lowest drought level (close to 0) and the Eastern Border sub-basin with the highest (around -0.1 to -0.2). Examining the periodic indices across the three decades highlights the temporal evolution of drought. The 2008-2017 period was marked by the most severe drought, with the Eastern Border sub-basin reaching an index of approximately -1. The Lake Urmia sub-basin, conversely, experienced the least severe drought during this period, with an index of around -0.5 to -0.6. In the preceding decade (1998-2007), the Persian Gulf and the Sea of Oman sub-basin suffered the most intense drought (around -1.2 to -1.3), while the Lake Urmia sub-basin again showed the least severe conditions (around -0.8 to -0.9). A similar pattern was observed in the earliest period (1988-1997), with the Persian Gulf and the Sea of Oman sub-basin experiencing the highest drought levels (around -0.8 to -0.9) and the Lake Urmia sub-basin the lowest (around -0.6 to -0.7). A clear and consistent trend emerges from this data: the Lake Urmia sub-basin consistently exhibits the lowest levels of drought compared to other regions. Conversely, the Eastern Border and Qara Qum sub-basins are persistently identified as experiencing the most severe drought conditions. This suggests that specific regional and climatic factors are at play in these areas, exacerbating the effects of drought. The study also indicates a general increase in drought severity over time, with the 2008-2017 period experiencing the most intense drought conditions. This temporal trend may be linked to broader global climate change patterns and rising temperatures, highlighting the need for further investigation into the relationship between large-scale climate variability and regional drought dynamics. This study investigated regional drought dynamics in Iran, analyzing the interplay between large-scale climate patterns and local conditions. A key finding is the overall trend towards wetter conditions, indicated by the dominance of "wet index" values. However, exceptions exist in the Eastern Border basin and Qarah-Qom region, which remained within normal ranges. The research reveals significant regional variations in drought severity. Using a combined Standardized Precipitation Index (SPI) and Southern Oscillation Index (SOI) for three months, the Caspian Sea sub-basin experienced the mildest drought (around -0.4), while the Qaraqorum sub-basin faced the most severe (between -0.5 and -0.6). A combined SPI and North Atlantic Oscillation (NAO) index showed similar trends, with the Lake Urmia sub-basin experiencing the least severe drought (near 0) and the Eastern Border sub-basin the most severe (between -0.1 and -0.2). Analyzing drought severity across three decades (1988-2017) provides further insights. The most recent decade (2008-2017) saw the Eastern Border sub-basin experiencing the most intense drought (around -1), while the Lake Urmia sub-basin had the least severe (between -0.5 and -0.6). In the preceding decade (1998-2007), the Persian Gulf and Sea of Oman sub-basin suffered the most severe drought (between -1.2 and -1.3), while the Lake Urmia sub-basin again showed the least severe conditions (between -0.8 and -0.9). The earliest period (1988-1997) also saw the Persian Gulf and Sea of Oman sub-basin with high drought severity (between -0.8 and -0.9), and the Lake Urmia sub-basin with the lowest (between -0.6 and -0.7). A consistent pattern emerges: the Lake Urmia sub-basin consistently experiences the lowest drought severity compared to other regions.

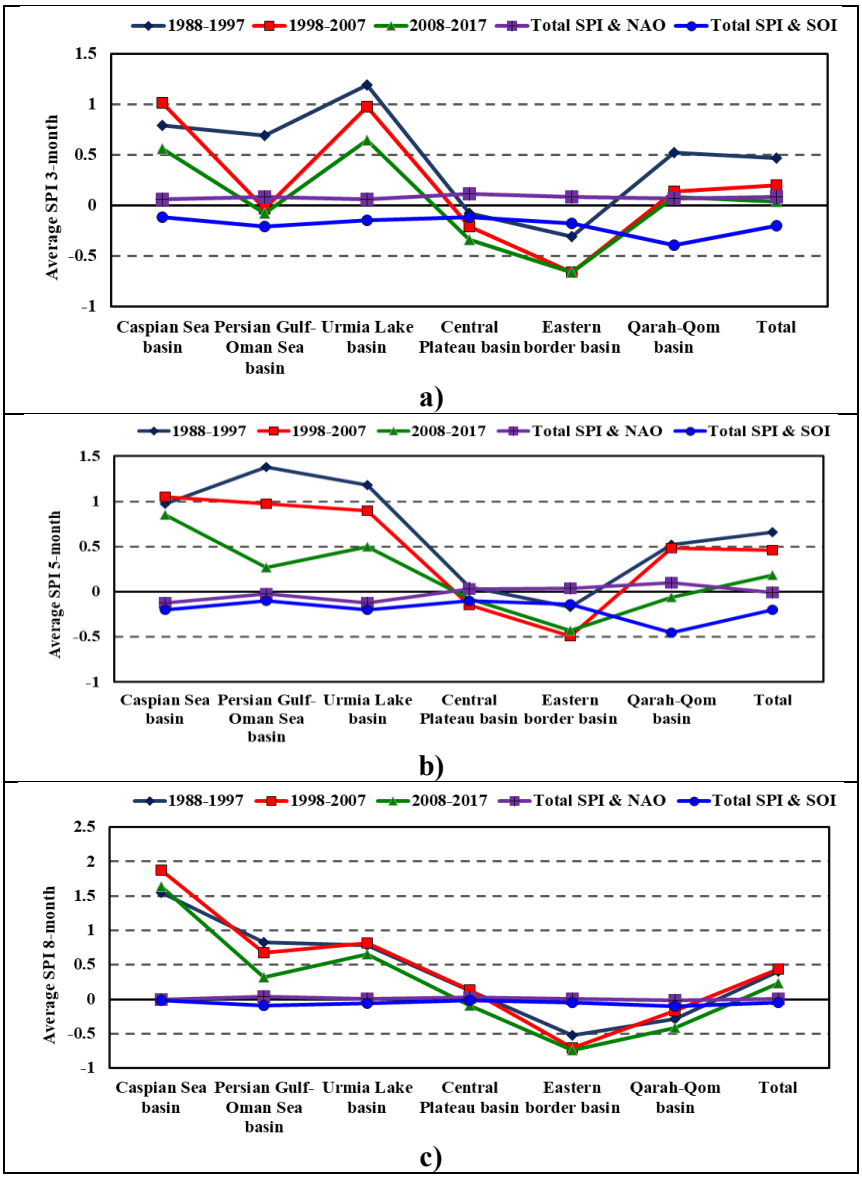

Figure 3. Average SPI values during three decades: A- Maximum SPI at a) time scale of 3 months, b) time scale of 5 months, c) time scale of 8 months

Conversely, the Eastern Border and Qaraqorum sub-basins consistently experience the most severe drought conditions, suggesting the influence of specific regional climatic factors. The data also suggests that the 2008-2017 period experienced generally more severe drought compared to the two preceding decades. This observation potentially links to global climate change and rising temperatures, which could be exacerbating drought conditions in specific regions of Iran. This study underscores the complex relationship between large-scale climate patterns and regional drought dynamics. It emphasizes the need for targeted water resource management and drought mitigation strategies tailored to the specific vulnerabilities of each sub-basin. Understanding these regional variations is crucial for effective planning and resource

allocation to minimize the impacts of drought. (Figure 4).

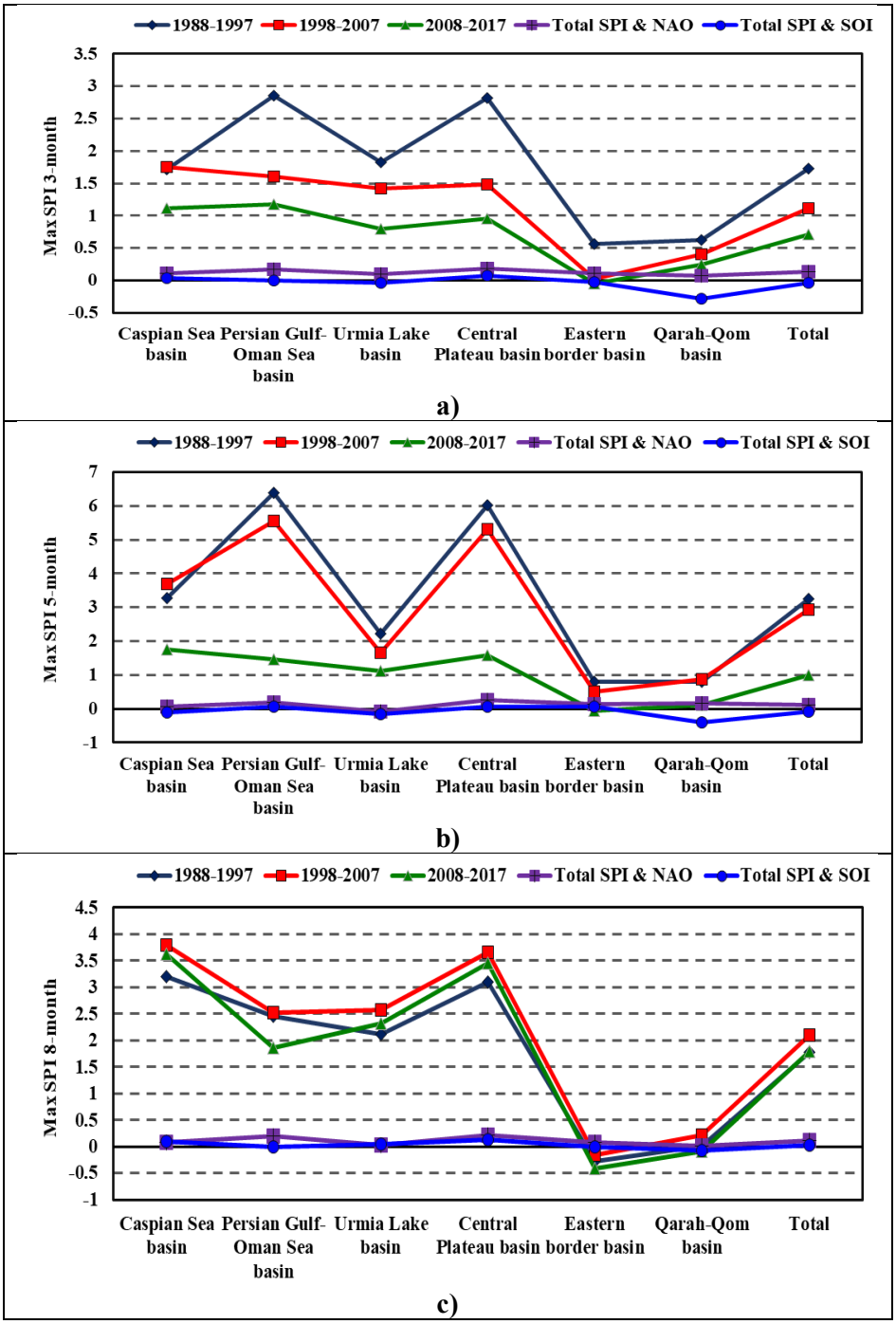

Figure 4. Maximum SPI values during three decades: A- Maximum SPI at a) time scale of 3 months, b) time scale of 5 months, and c) time scale of 8 months

The research reveals distinct drought patterns across three time periods: 1988-1997, 1998-

2007, and 2008-2017. From 1988 to 1997, the most severe drought was concentrated in the southern and southeastern regions, specifically within the Persian Gulf and the Sea of Oman, and the Eastern Border sub-basins. These areas experienced intense and widespread drought. Conversely, the central and northwestern regions, notably the Lake Urmia sub-basin, experienced less severe conditions. The period from 1998 to 2007 witnessed an intensification of drought across Iran. While the southern and southeastern regions continued to endure high severity, the drought gradually expanded towards the central areas. Although the Lake Urmia sub-basin remained relatively less affected compared to other regions, it too experienced an increase in drought conditions. The most severe drought period occurred between 2008 and 2017. During this decade, drought engulfed nearly all parts of Iran. The southern and southeastern regions experienced extremely high severity, while the central and northwestern regions also saw a sharp rise in drought intensity. Critically, the Lake Urmia sub-basin, which had previously been relatively less affected, faced severe drought, indicating a significant deterioration. The study also examined the influence of large-scale climate patterns on regional drought. The combined SPI and SOI analysis revealed that the drought patterns largely mirrored those observed in the individual periods. However, it also highlighted the role of the SOI in exacerbating drought, particularly in the southern and southeastern regions. The SPI and NAO analyses showed a more complex relationship. The NAO's impact on drought varied regionally, intensifying drought in some areas and mitigating it in others. Overall, the influence of the NAO on drought was less pronounced than that of the SOI. A consistent pattern emerged throughout the study period. The Lake Urmia sub-basin consistently exhibited the lowest drought severity among the six sub-basins. Conversely, the Eastern Border and Qaraqum sub-basins consistently experienced the highest drought levels. This suggests that specific regional and climatic factors within these areas play a crucial role in driving drought conditions. The overall trend indicates a progressive increase in drought severity across Iran. The 2008-2017 period experienced significantly more severe drought compared to the previous two decades. This observation aligns with global climate change trends and rising temperatures, suggesting a potential link between global warming and regional drought intensification. The results from 2013 onwards, however, indicated a return to normal drought conditions in Iran. In summary, this research provides valuable insights into the spatial and temporal dynamics of drought in Iran. The analysis highlights the influence of large-scale climate patterns, such as SOI and NAO, on regional drought, as well as the importance of local climatic factors. The findings underscore the need for effective water resource management and drought mitigation strategies to address the increasing challenges posed by climate change and its impact on regional water availability (Figures 2, 3, 4).

The presented maps (Figures 5, 6, 7) illustrate the Standardized Precipitation Index (SPI) for three consecutive ten-year periods (1987-1997, 1998-2007, and 2008-2017) across the sub-basins of Iran. The SPI is a crucial indicator for drought monitoring, calculated using precipitation data and comparing it to the long-term average. Positive SPI values indicate wet periods, while negative values signify drought conditions. During the 1987-1997 period, vast areas of Iran, particularly the central and southern regions, experienced severe drought (SPI less than -1). The drought's intensity in some locations was so extreme that the SPI reached below -2, indicating extremely severe drought.

Conversely, certain northern and western parts of the country experienced wet conditions (SPI greater than 1). In the 1998-2007 period, the pattern of drought and wetness shifted. The central and southern regions of the country continued to face drought, but its severity decreased compared to the previous period. In contrast, the eastern regions of the country, especially the Sistan and Baluchestan province, faced severe drought. On the other hand, the northern and western regions of the country, particularly the Caspian Sea coasts, experienced wet conditions. During the 2008-2017 period, the drought gradually receded from the country, and conditions improved. However, some southern and eastern regions of the country still experienced mild to moderate drought. In contrast, the northern and western regions of the country, especially the East and West Azerbaijan provinces, experienced wet conditions. The examination of SPI maps reveals that Iran has experienced significant fluctuations in precipitation status over the past three decades. The severe droughts in the 1980s and 1990s posed serious challenges to the country. However, in the 2000s, conditions improved, and the drought gradually decreased. Nevertheless, it remains necessary to develop plans to address potential droughts in the future.

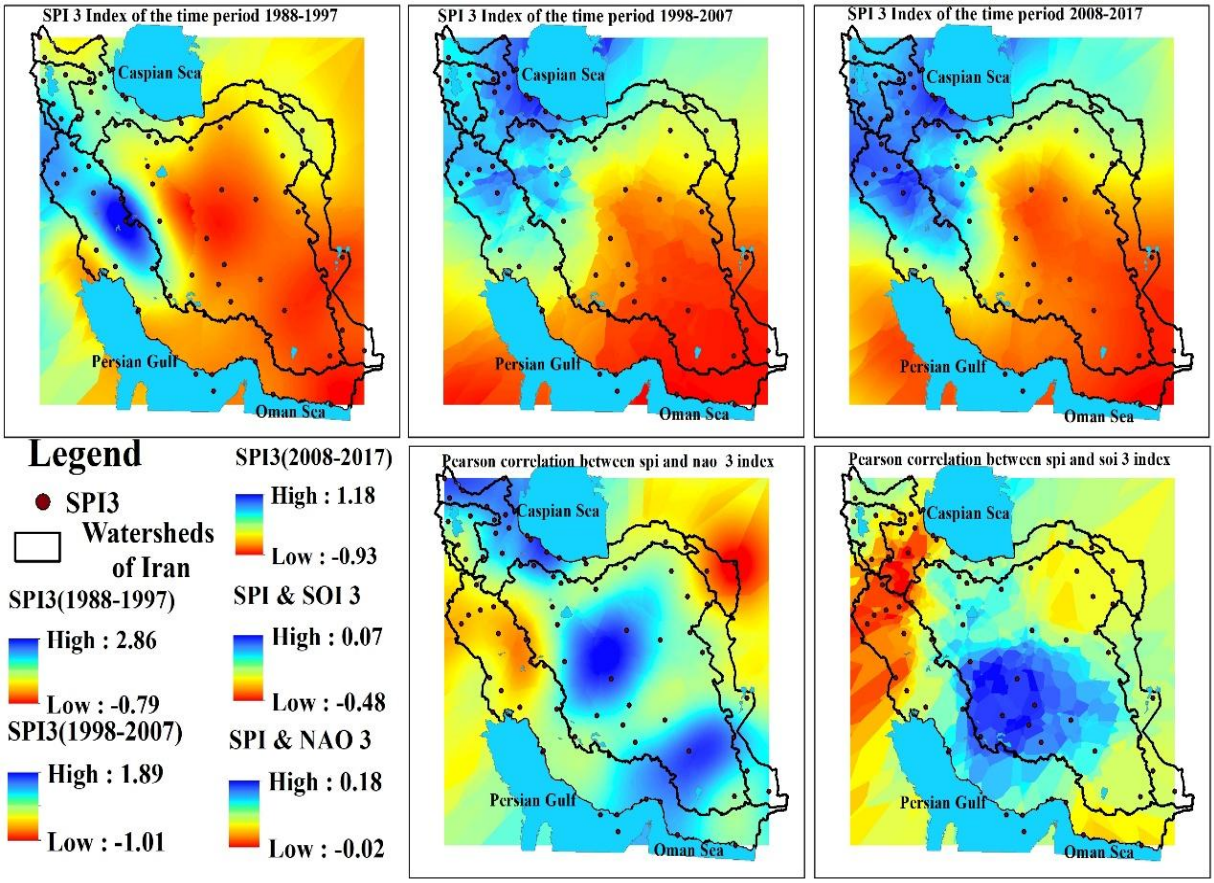

Figure 5. Standardized Precipitation Index map and NAO and SOI in the spring rainfall period (3 months)

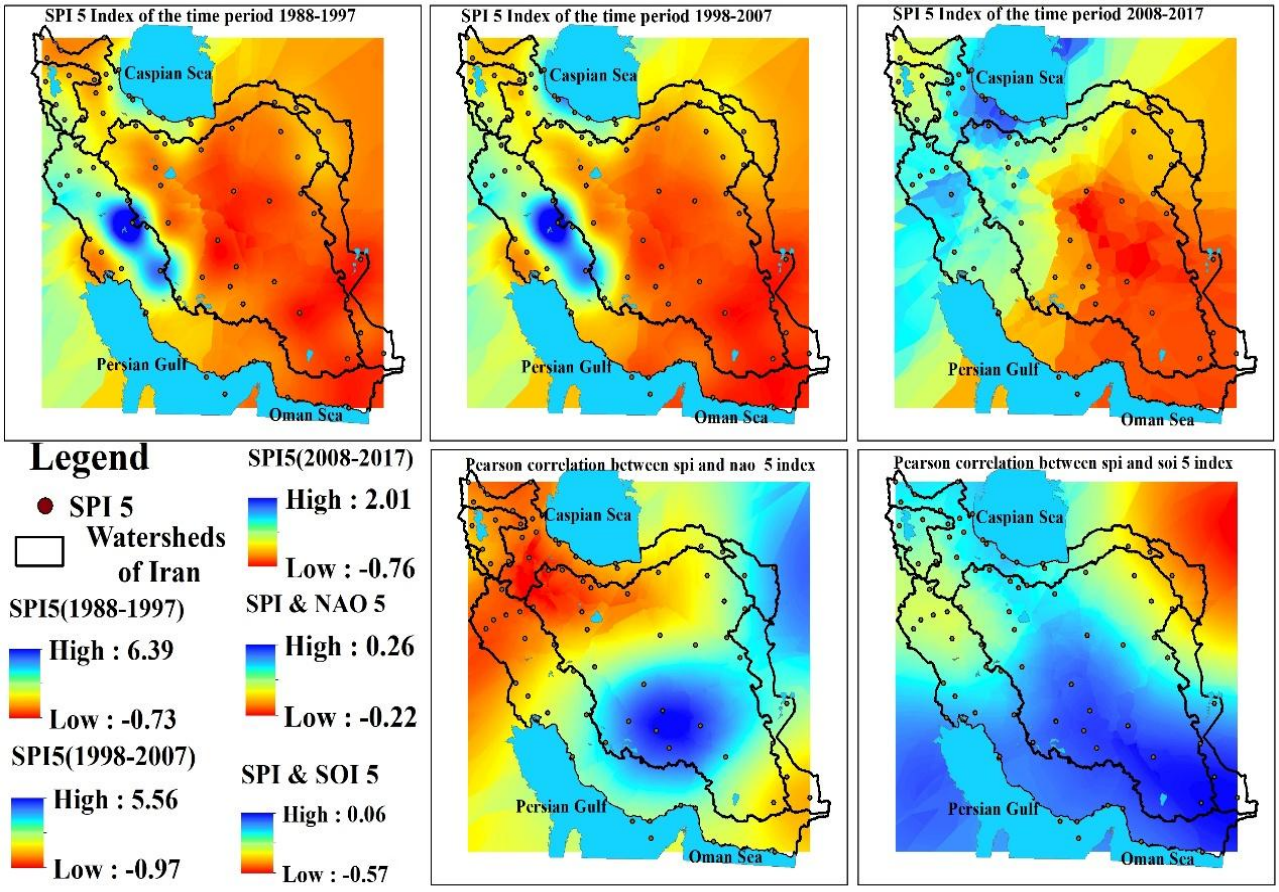

Figure 6. Standardized Precipitation Index map, and NAO and SOI During the Winter and Spring Rainfall (5 months)

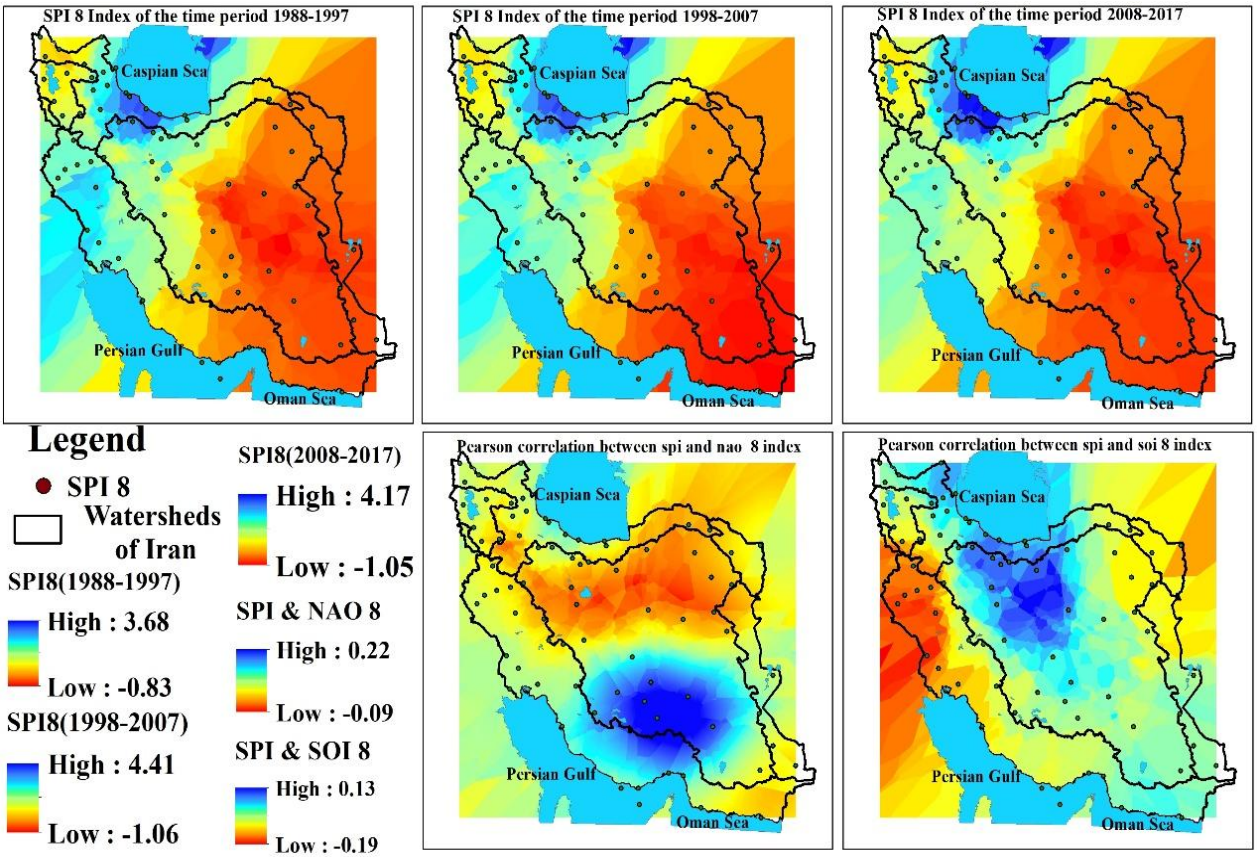

Figure 7. Standardized Precipitation Index Map and NAO and SOI during the Annual Rainfall Period (8 months)

3.1. SOI VS. Drought Analysis

The Pearson correlation coefficient was calculated between the monthly SPI in the periods of 3, 5, and 8 months until the end of May and the SOI signals. The results are listed in Table 3. For the months March, April, and May (a 3-month period), SPI at Sarakhs station showed a significant correlation coefficient of -0.54 with SOI signals. In this period, the SPI at Mashhad, Koohrang, Aligudarz, and Ilam stations also showed a significant (at the level of 0.05) correlation coefficient of -0.41, -0.45, -0.41, and -0.38, respectively, with the SOI signals. Based on the 3-month period analysis, SPI in other stations was not significantly correlated with SOI signals. Based on the 5-month.

The Pearson correlation coefficient matrix was calculated between the standard monthly precipitation index of SPI stations in the periods of 3, 5, and 8 months until the end of May and the SOI signals. The results are listed in Table 3. The results for March, April, and May (3-month period) show that the SPI index of Sarakhs station showed for 3 months with a significant correlation coefficient of -0.54 at the level of one percent, indicating a negative and significant correlation with SOI signals., In this period, the SPI at Mashhad, Koohrang, Aligudarz, and Ilam stations also showed a significant (at the level of 0.05) correlation coefficient of -0.41, -0.45, -0.41, and -0.38, respectively, with the SOI signals (at the 5% level). Based on the 3-month analysis, SPI in other stations was not significantly correlated with SOI signals. Also, in the 5-month based on 5-month analysis, SPI in Sarakhs station showed a correlation coefficient of -0.63 (at the level of

one percent0.01) with SOI signals, indicating a negative and significant correlation. At the same time, SPI in Mashhad station, with a correlation coefficient of -0.51, has had a negative and significant correlation with SOI signals (at the level of one percent). The SPI at the stations of Torbat Heydariyeh, Quchan, Kashmar, Tabriz, Koohrang, Kangavar, and Khorramabad also shows the correlation coefficients of -0.37, -0.44, -0.41, -0.38, -0.36, -0.40, and -0.34 (significant at the level of 0.05), respectively, have a negative and significant correlation with SOI symptoms signals, respectively (at the level of 5%). Also, based on the 8-month analysis, SPI in Shahroud station with negative coefficients of -0.34 at the 5% level has a negative and significant correlation relationship with SOI signals.

According to Table 3, which is based on the 33-monthly analysis, about 15% of Iranian study stations were affected by spring rains precipitations with the intensity of Walker streams (La-Niña). 85% of total stations were affected by the weakening of Walker streams (El-Niño), as well. The according to the 5-5-monthsanalysis, about 19% of Iran's the study stations were affected impacted by heavy rainfalls in the first rainfall of the year (the first of early winter) and by the end of spring with the intensity of Walker (La-Niña) streams at the end of spring, and 81% percent of total stations were affected by the weak Walker streams (El-Niño).

Based on the 8-month analysis, about 42% of Iran's study stations showed a correlation between annual rainfall and the intensification of Walker circulation associated with La-Niña. Additionally, 58% of the country's stations were affected by the weakening of the Walker circulation linked to El-Niño. In general, by examining the studied stations, it can be stated that SOI signals have a contribution an effect of 42% on annual droughts in Iran, but in spring rainfall and the rainfalls of the early year (early winter) to late spring, we cannot observe a significant show the low impact of La-Niña phenomenon on Iran. SimilarlyHowever, it can be said that most of the El-Niño phenomenon mostly affects Iran's droughts and rainfalls period analysis, SPI in Sarakhs station, showed a correlation coefficient of -0.63 (at the level of one percent0.01) with SOI signals has a negative and significant correlation. At the same time, SPI in Mashhad station, with a correlation coefficient of -0.51, has had a negative and significant correlation with SOI signals (at the level of one percent). The SPI at the stations of Torbat Heydariyeh, Quchan, Kashmar, Tabriz, Koohrang, Kangavar, and Khorramabad also shows the correlation coefficients of -0.37, -0.44, -0.41, -0.38, -0.36, -0.40, and -0.34 (significant at the level of 0.05), respectively, indicating a negative and significant correlation with SOI symptom signals (at the 5% level). Also, based on the 8-month analysis, SPI in Shahroud station with negative coefficients of -0.34 at the 5% level has a negative and significant correlation with SOI signals.

According to Table 3, which is based on the 3-month analysis, about 15% of Iranian study stations were affected by spring rains precipitations with the intensity of Walker streams (La-Niña). 85% of total stations were affected by the weakening of Walker streams (El-Niño), as well. The according to the 5-5-monthsanalysis, about 19% of Iran's the study stations were affected impacted by heavy rainfalls in the first rainfall of the year (the first of early winter) and by the end of spring with the intensity of Walker (La-Niña) streams at the end of spring, and 81% percent of total stations were affected by the weak Walker streams (El-Niño) .

Based on the 8-month analysis, about 42% of Iran's study stations showed a significant correlation between annual rainfall and the intensification of the Walker circulation (La-Niña). Additionally, 58% of the country's stations were affected by the weakening of

the Walker circulation (El-Niño). In general, by examining the studied stations, it can be stated that SOI signals have a contribution an effect of 42% on annual droughts in Iran, but in spring rainfall and the rainfalls of the early year (early winter) to late spring, we cannot observe a significant show the low impact of La-Niña phenomenon on Iran. However, it can be said that most of the El-Niño phenomenon mostly affects Iran's droughts and rainfalls. SOI data indicates that Iran has been affected by climatic fluctuations over different periods. The El Niño phenomenon appears to have a greater impact on the country's climate in 5- and 8-month periods. SPI maps show that Iran has experienced significant fluctuations in precipitation over the past three decades. Severe droughts in the 1980s and 1990s have posed serious challenges to the country. However, in the 2000s, conditions improved, and drought gradually decreased. Nevertheless, it is still necessary to make the necessary plans to deal with possible droughts in the future. The examination of SOI data and SPI maps shows that Iran has been affected by climatic fluctuations and drought over different periods. It seems that the El Niño phenomenon and climate change have affected rainfall and drought patterns in Iran.

Table 3. Correlation of monthly precipitation at the studied stations with the SOI and drought-related climate variability

Station	3-months	5-months	8-months	Station	3-months	5-months	8-months	Station	3-months	5-months	8-months
Torbat Heydarieh	-0.29	-0.37*	-0.19	Gharakheil	-0.23	-0.22	0.06	Kashan	-0.08	0.04	0.32
Sabzevar	-0.08	-0.21	0.19	Nowshahr	-0.04	-0.03	0.10	Jask	-0.06	-0.16	-0.11
Sarakhs	-0.54**	-0.63**	-0.37	Astara	0.02	-0.13	0.07	Bandar Abbas	-0.05	0.02	-0.12
Ferdows	-0.07	-0.10	0.04	Bandar Anzali	0.00	0.21	0.33	Bandar Lengeh	-0.09	-0.15	-0.12
Quchan	-0.27	-0.44*	0.02	Rasht	-0.03	-0.13	0.08	Kish Island	-0.14	-0.05	-0.05
Kashmar	-0.32	-0.41*	-0.20	Ardabil	-0.09	-0.31	-0.04	Minab	-0.05	0.04	0.04
Mashhad	-0.40*	-0.51**	-0.19	Pars Abad	-0.06	-0.12	0.13	Abadeh	-0.08	0.04	-0.03
Bojnord	-0.29	-0.35	-0.14	Khalkhal	-0.13	-0.30	-0.06	Shiraz	-0.25	-0.05	-0.12
Birjand	-0.21	-0.32	-0.16	Ahar	0.05	-0.06	0.17	Bushehr	-0.17	-0.04	-0.12
Iranshahr	-0.20	0.10	0.13	Tabriz	-0.30	-0.38*	-0.21	Shahr-Kord	-0.26	-0.22	-0.12
Chabahar	-0.19	-0.01	-0.02	Sarab	0.02	-0.09	0.08	Kouhrang	-0.45*	-0.36*	-0.28
Khash	-0.18	0.11	0.10	Mianeh	-0.02	-0.21	-0.04	Hamadan	-0.33	-0.32	0.09
Zabul	-0.27	-0.32	-0.27	Urmia	-0.12	-0.17	-0.01	Islamabad Gharb (West Islamabad)	-0.34	-0.36	-0.26
Zahedan	0.04	0.21	0.05	Khoy	0.05	-0.06	-0.04	Kangavar	-0.34	-0.40*	-0.18
Saravan	-0.07	0.10	0.05	Maku	-0.01	-0.13	0.02	Kermanshah	-0.26	-0.27	-0.11
Anar	-0.13	-0.02	-0.07	Mahabad	-0.27	-0.28	-0.18	Aligoudarz	-0.41*	-0.31	-0.17
Bam	0.08	0.02	0.02	Ab-ali	-0.22	-0.28	0.07	Khorramabad	-0.32	-0.34*	-0.20
Sirjan	-0.06	0.07	-0.12	Tehran-Mehrabad	-0.12	-0.19	0.12	Ilam	-0.38*	-0.25	-0.29
Shahre-Babak	-0.23	-0.03	-0.14	Karaj	-0.14	-0.14	0.20	Qom	-0.23	-0.15	0.23
Kerman	-0.23	0.03	-0.02	Qazvin	0.04	-0.11	-0.12	Abadan	-0.27	-0.02	-0.08
Tabas	-0.19	-0.12	0.02	Khorramdarreh	-0.14	-0.26	-0.06	Omīdīyeh	-0.32	-0.09	-0.19
Yazd	0.08	0.11	0.30	Zanjan	-0.05	-0.18	-0.01	Ahvaz	-0.28	-0.03	-0.19
Shahrood	-0.23	-0.30	-0.34*	Saghez	-0.27	-0.27	-0.22	Bostan	-0.19	-0.09	-0.16
Semnan	-0.18	-0.17	0.13	Sanandaj	-0.24	-0.32	-0.20	Takab	-0.09	-0.14	-0.24
Babolsar	-0.15	-0.06	0.06	Isfehan	-0.08	-0.13	0.04	Abu Musa island	-0.05	0.01	0.06
Ramsar	0.17	-0.04	-0.21	Khor Biabanak	0.07	0.03	0.21	Djolfa	0.05	-0.07	0.05
** Significance at 1% level, * Significant at 5% level								Yasuj	-0.11	-0.05	0.10

3.2. NAO VS. Drought Analysis

In this study, determining the severity of drought in the country's stations, a correlation matrix was formed to investigate the effect of the NAO phenomenon on the occurrence of drought and wet periods in Iran. The Pearson correlation coefficient matrix was calculated between the standard monthly precipitation index SPI of the selected stations in the period of 3, 5, and 8 months until the end of May(Table 4). Based on the 3-month analysis, the SOI signal results are listed in Table 4. The results for March, April, and May, which could be revealed (3-month), show that the correlation between the SPI index at all stations in the country with NAO signals was not significant. However, according to the 5-month analysis, the Shahre-Babak station, with a correlation coefficient of 0.39 at the level of 5% had established a positive and significant correlation relationship (at the level of 0.05) with NAO signals. In the same period, the Qazvin station in the same period with a correlation coefficient of -0.43 (significant at 5% level), showed a negative relationship and significant correlation with NAO signals. Furthermore, based on the 8-month analysis on Bam and Ramsar stations, both of them with the correlation coefficients of 0.36 (significant at 5% level), demonstrated a positive and significant correlation relationship with NAO signals. According to Table 4, over a 3-month period, about 27% of Iranian studied stations have had relatively little contact with high-pressure as well as low-pressure Icelandic (low-pressure gradients) due to spring precipitation. On the other hand, 73% of the stations were affected by the excessive pressure in the Azure high-pressure and less than the normal pressure in low-pressure Iceland (high-pressure gradient between the two centers).

Based on the 5-month analysis, about 66% of the Iranian stations had relatively high levels of correlation between rainfall with the first precipitation of the year (first early winter) until the end of spring, and with high pressure near the weak tropics as well as low-pressure Icelandic (low-pressure gradient). About 34% of the studied stations were affected by the excessive pressure in the Azure high pressure and less than normal pressure in the Icelandic low pressure (high-pressure gradient between the two centers)[MR2]. According to the 8-month analysis, about 44% of the selected Iranian stations showed a relatively low-to-medium correlation between annual rainfall and high-pressure Azure, as well as Icelandic low-pressure gradients. Moreover, 56% of the stations were affected by the excessive pressure in the Azure high-pressure and less than the normal pressure in the low-pressure Iceland (high-pressure gradient between the two centers). Overall, the signals of the NAO were significantly affected by the annual precipitation in Iran under the influence of excessive pressure in the Azure high-pressure and less than normal pressure in the Icelandic low-pressure system (high-pressure gradient between the two centers). Based on the 5-month analysis, 66% of the studied stations were affected by the high pressure near the weak tropics, as well as the low-pressure Icelandic (low-pressure gradient). This study investigated the influence of global meteorological signals, specifically the Southern Oscillation Index (SOI) and the North Atlantic Oscillation (NAO), on drought occurrence in Iran, utilizing the Standardized Precipitation Index (SPI) to characterize drought conditions. Analysis of rainfall data from 79 synoptic stations across Iran, spanning 1988 to 2017, revealed complex spatial and temporal patterns of drought. Our findings indicate a general trend of mild to moderate droughts across the country, except for the Lake Urmia basin, which experienced relatively wetter conditions. Notably, the Central Plateau and Eastern Border regions exhibited particular vulnerability to drought, especially during the 1998-2007 period. While the minimum SPI analysis suggested a country-wide susceptibility to drought, the mean SPI analysis highlighted the eastern border region as being consistently affected, with milder drought conditions observed in the Central Plateau and Qarah-Qom regions. The analysis of SPI coupled with SOI and NAO revealed varying degrees of correlation across different sub-basins and time scales, suggesting a complex interplay between these global climatic drivers and regional drought patterns.

Table 4. Correlation of monthly precipitation at the studied stations with the NAO and drought-related climate variability.

Station	3-months	5-months	8-months	Station	3-months	5-months	8-months	Station	3-months	5-months	8-months
Torbat Heydarieh	-0.02	-0.03	-0.10	Gharakheil	0.19	0.03	-0.05	Kashan	0.20	-0.15	-0.22
Sabzevar	0.11	-0.14	-0.11	Nowshahr	0.23	-0.07	0.14	Jask	-0.05	0.04	-0.06
Sarakhs	0.18	0.28	0.20	Astara	0.15	-0.06	0.19	Bandar Abbas	0.14	0.05	0.13
Ferdows	0.18	0.14	0.01	Bandar Anzali	0.22	-0.07	0.18	Bandar Lengeh	0.07	0.09	0.07
Quchan	0.06	-0.05	-0.09	Rasht	0.13	-0.03	0.16	Kish Island	0.02	0.13	0.08
Kashmar	0.08	0.09	0.06	Ardabil	-0.13	-0.11	0.09	Minab	-0.06	-0.01	0.18
Mashhad	0.02	0.12	0.03	Pars Abad	-0.08	-0.17	0.04	Abadeh	0.21	0.17	0.11
Bojnord	0.05	0.02	-0.11	Khalkhal	-0.05	-0.26	-0.19	Shiraz	0.22	0.12	0.15
Birjand	0.09	0.02	-0.20	Ahar	0.18	-0.18	0.06	Bushehr	0.03	0.00	0.03
Iranshahr	0.07	-0.18	-0.20	Tabriz	0.34	0.13	0.25	Shahr-Kord	0.04	-0.10	-0.12
Chabahar	0.15	0.00	-0.05	Sarab	-0.10	-0.25	-0.26	Kouhrang	0.16	0.00	0.08
Khash	0.04	-0.11	-0.09	Mianeh	-0.08	-0.26	-0.15	Hamedan	0.22	-0.16	-0.16
Zabul	0.07	0.15	0.11	Urmia	0.11	-0.02	-0.02	Islamabad Gharb (West Islamabad)	0.01	-0.18	0.09
Zahedan	0.11	-0.04	0.11	Khoy	0.28	-0.10	0.24	Kangavar	-0.02	-0.22	0.01
Saravan	0.04	-0.13	-0.04	Maku	0.30	-0.20	-0.06	Kermanshah	-0.03	-0.23	-0.05
Anar	0.28	0.35	0.28	Mahabad	0.13	-0.07	0.03	Aligoudarz	0.16	-0.04	0.01
Bam	0.10	0.21	0.36*	Ab-ali	0.04	-0.16	0.01	Khorramabad	-0.05	-0.11	-0.03
Sirjan	0.13	0.19	0.27	Tehran-Mehrabad	0.04	-0.27	-0.11	Ilam	-0.08	-0.17	0.11
Shahre-Babak	0.34	0.39*	0.32	Karaj	0.05	-0.31	-0.04	Qom	0.24	-0.10	-0.05
Kerman	0.17	0.28	0.19	Qazvin	-0.14	-0.43*	-0.02	Abadan	-0.02	-0.08	0.02
Tabas	0.04	-0.01	-0.23	Khorramdarreh	-0.07	-0.23	-0.04	Omīdīyeh	0.03	0.18	0.20
Yazd	0.09	0.27	0.13	Zanjan	0.10	-0.14	-0.04	Ahvaz	0.08	-0.13	0.03
Shahrood	-0.03	-0.12	0.14	Saghez	-0.03	-0.10	0.06	Bostan	-0.13	-0.18	0.02
Semnan	0.04	-0.15	-0.18	Sanandaj	0.01	-0.09	-0.07	Takab	-0.08	-0.26	0.01
Babolsar	0.12	-0.08	-0.02	Isfehan	0.17	0.08	0.04	Abu Musa island	-0.08	-0.21	-0.28
Ramsar	0.18	0.17	0.36*	Khor Biabanak	-0.01	-0.20	-0.15	Djolfa	0.12	-0.27	-0.11
* Significant at 5% level								Yasuj	0.25	-0.01	-0.11

The observed temporal variations in drought severity underscore the need for continuous monitoring and further research to fully understand the complex interaction between global climate signals and regional drought dynamics in Iran.

These findings contribute valuable insights for water resource management and drought mitigation strategies in this arid and semi-arid region, emphasizing the importance of incorporating large-scale climate variability into regional planning efforts. Further research could explore the specific mechanisms through which SOI and NAO influence Iranian precipitation patterns, potentially leading to improved drought forecasting and preparedness. Continued research and innovation in drought analysis are essential to address existing challenges and further our understanding of drought dynamics. This includes improving monitoring and forecasting capabilities, and enhancing resilience and adaptation strategies against drought. Considering the temporal behavior of the percentage of rain gauges indicating drought conditions and trend analysis, the results of this study are consistent with other studies conducted on drought characterization in the Mediterranean region. The spatial and temporal extent of drought events in the study area showed that most drought events were observed between 1997 and 2007. These results corroborate the findings reported by Hoerling et al. (2012), which indicated an increase in drought periods during the first decade of the 2000s, and also align with those of Spinoni et al. (2015), Kenawy et al. (2025), who identified the highest frequency, duration, and intensity of droughts as occurring in the 1990s and 2000s. Furthermore, the period under investigation encompasses two of the most

extensive and devastating droughts of the past 40 years in the Mediterranean basin (i.e., 1999-2001 and 2007-2012) (Mathbout et al., 2021). In this paper, the observational period has been extended to the end of 2017. Indeed, while the overall trends remain consistent, varying proportions of stations exhibiting significant trends have been observed. Nevertheless, the results of this study, which reveal a decrease in SPI values during winter, in wet months, and on an annual scale, and an increase in SPI values during summer, confirm the tendency towards decreasing winter and annual precipitation and increasing summer precipitation identified in several regions of Iran (Caloiero and Veltri, 2019). Ultimately, the results of this study confirm that the temporal evolution of drought in the Mediterranean region, and specifically in the study area, is typically associated with changes in the intra-annual distribution of rainfall and is therefore related to some teleconnection patterns (Caloiero et al., 2021; Holgate et al., 2025; Xu et al., 2025). Drought in this region is mainly influenced by the North Atlantic Oscillation (NAO) and, to a lesser extent, by other teleconnection patterns such as the El Niño-Southern Oscillation (ENSO) (Loyd-Huhes and Saunders, 2002). Specifically, in the study area, strong positive phases of the NAO tend to be associated with below-normal temperatures and below-normal precipitation, while opposite patterns of temperature and precipitation anomalies are 1 commonly observed during strong negative phases of the NAO (Caloiero et al., 2011). These results, which demonstrate the link between NAO phases and drought periods in the Calabria region, corroborate previous studies conducted in the Mediterranean area. Indeed, several authors have acknowledged that the NAO is largely responsible for drought periods in this region (e.g., Vicente-Serrano et al., 2011). For instance, as shown by Kelley et al. (2012), a distinct negative phase of the NAO occurred between 1940 and 1980, and consequently, this period is characterized by above-average rainfall in the Mediterranean basin and positive values of the Standardized Precipitation Index (SPI). Conversely, the dry conditions observed at the beginning of this century correspond to a positive phase of the SPI. Regarding ENSO, the weak influence of this teleconnection pattern on the rainfall of the Calabria region has been identified in previous studies (Caloiero et al., 2011), although it has been recognized as one of the main drivers of drought events in other regions such as Turkey (Abdelkader et al., 2022) or China (Yang and Xing, 2022). In addition to the SOI and NAO, which represent large-scale atmospheric behavior, the results of this study showed the strong influence of the Mediterranean Oscillation (MO), thus confirming the findings of Mathbout et al. (2021). The results of this study highlight the increasing signals of climate change in meteorological drought. Precipitation deficits can be amplified through a positive feedback loop. In this loop, dry soil and reduced vegetation cover increase surface albedo, limit evapotranspiration, and increase surface heating. As a result, meteorological drought is exacerbated (Taylor et al., 2002; Dai et al., 2018). Changes in soil moisture and runoff are mainly caused by changes in precipitation and evapotranspiration (Zhao and Dai, 2022). Changes in all features of meteorological and hydrological droughts are found in some areas of the Northern Hemisphere, such as North America, Europe, and Central Asia. These areas are mainly snow-dominated, where snow dynamics are important. In these regions, changes caused by global warming in the timing of snowmelt (Musselman et al., 2017), snow water equivalent (Shi and Wang, 2015), and snow-rain partitioning (Burn and Whitfield, 2016) play a pivotal role. Similarly, changes in floods in these areas will not follow changes in heavy precipitation due to the role of snow dynamics (Tabari, 2021). In this study, the magnitude of trends in behavioral series composed of SPI values was assessed. As defined by Brasil Neto et al. (2021), changes in behavioral series occur monthly and reflect monthly changes in SPI values. Negative trends in behavioral series indicate a scenario of increasing drought magnitude. This finding is consistent with the expectations and discussions of various researchers that, with the shortening of the precipitation accumulation period, the SPI series becomes more sensitive to changes in rainfall events, leading to more frequent alternations between wet (SPI > 0) and dry (SPI ≤ 0) events (Brasil Neto et al., 2020; Santos et al.,

2020; Brasil Neto et al., 2021; Brasil Neto et al., 2022).

In this study, two important factors in droughts can be discussed that are not within the scope of this study. First, is the effective role of human activities (Van Loon et al., 2016; Tijdeman et al., 2018; AghaKouchak et al., 2021; Li et al., 2021). Human management of the landscape, through hydraulic structures and land use change, profoundly affects water dynamics across various landscape components. These interventions are often local or regional in scale. To incorporate anthropogenic effects into drought analyses, additional data such as records of management actions should be considered. However, at the scale of analysis in this study, the effects of deep human intervention are beyond the scope of investigation. The second factor is seasonal snow storage, which has a profound impact on the drought cascade (Van Loon & Van Lanen, 2012; Van Loon et al., 2014; Apurv et al., 2017; Huning & AghaKouchak, 2020). Snowpacks link winter precipitation to warm-season streamflow and soil moisture deficits, and as such, are essential components of drought cascades. In this study, snow water storage is not considered as a separate component of the cascade. To incorporate snow droughts and their role in the drought cascade, seasons should be analyzed specifically and separately. Although the role of snow in the regional water balance is important, the approach of this study cannot provide the necessary analytical framework to understand its influence. Finally, drought termination due to displacement events such as cyclones and atmospheric rivers is another dimension of drought studies, which depends on regional climates and the degree of correlation with larger-scale ocean-atmosphere interactions (Wu & Dirmeyer, 2020).

4. Conclusions

This study investigated the influence of global meteorological signals, specifically the Southern Oscillation Index (SOI) and the North Atlantic Oscillation (NAO), on drought occurrence in Iran. Using the Standardized Precipitation Index (SPI), calculated from 79 synoptic stations across Iran over three decades (1988-2017), the research explored the complex interaction between these large-scale climate patterns and regional drought dynamics. The analysis considered various timescales (3, 5, and 8 months) and six distinct sub-basins, providing a detailed understanding of drought variability nationwide. Analysis of minimum SPI values revealed fluctuating drought trends. While the Lake Urmia basin remained largely unaffected, experiencing near-normal to slightly wet conditions, other regions showed significant variations in drought severity. A general trend of shifting drought patterns emerged across the three decades. Initially (1988-1997), mild droughts were prevalent, with the Central Plateau experiencing the most severe conditions. This was followed by an intensified drought (1998-2007), impacting the entire country, again with the Central Plateau most affected. Finally, a decrease in severity was observed (2008-2017), with a return to mild drought in most regions. This temporal variability highlights the dynamic nature of drought and the need for ongoing monitoring. Composite indices of SPI with SOI and NAO revealed distinct regional patterns. The SPI-SOI index indicated that the Caspian Sea sub-basin experienced the least severe drought, while the Qaraqum sub-basin suffered the most. Similarly, the SPI-NAO index showed the Lake Urmia sub-basin with the lowest drought severity and the Eastern Border sub-basin with the highest. These regional differences demonstrate varying sensitivities to these global climate signals. Periodic indices for each decade further emphasized these regional and temporal variations. The Eastern Border and Qaraqum sub-basins consistently exhibited higher drought severity, and the periods 1998-2007 and 2008-2017 experienced more intense drought than 1988-1997. Analysis of mean SPI changes reinforced the trend of increasing drought, particularly in the eastern border region. During the second and third decades, this region experienced significant drought, with the Central Plateau and Qaraqum also showing signs of mild drought. This eastward expansion raises concerns about long-term water security. Conversely, the earlier period (1988-1997) saw mild drought in the Eastern Iranian border basin, while other regions experienced near-normal to slightly wet conditions. This temporal shift suggests the potential influence of climate change on regional drought patterns. The study explored the

influence of SOI and NAO. The SOI, reflecting El-Niño-Southern Oscillation, significantly exacerbated drought, particularly in southern and southeastern Iran. The NAO, however, had a more complex and regionally varying influence, with a less pronounced overall impact. These findings emphasize the importance of understanding the individual and combined effects of these climate signals for accurate drought prediction and mitigation. Spatial distribution of SPI across the three decades, visualized through maps, further supported the observed trends. The maps clearly illustrated shifting drought patterns, with southern and southeastern regions initially most affected, followed by expansion towards central areas, and finally, a general intensification across most of the country, including the previously less affected Lake Urmia sub-basin. These visual representations are effective visualizations for communicating drought risk and informing decision-making. In conclusion, this study provides valuable insights into the complex relationship between global meteorological signals and regional drought dynamics in Iran. The findings underscore the importance of considering both SOI and NAO, along with regional climatic factors, for a comprehensive understanding of drought. Observed trends of increasing drought severity, particularly in eastern regions, highlight the need for proactive water resource management and effective drought mitigation strategies. Further research, incorporating climate models and advanced statistical techniques, is crucial for improving drought prediction and building resilience to future climate change impacts. This information is crucial for policymakers, water resource managers, and communities in developing sustainable strategies for adapting to and mitigating drought effects in Iran. Improvements to this study could involve analyzing different types of drought in the wider region, taking into account, for example, remote sensing (Zhao et al., 2018), which can provide valuable information, especially for areas with limited ground-based observations. Furthermore, future research could focus on various methods such as machine learning models (Wang et al., 2022; Sattari et al., 2020). Based on findings revealing the Eastern Border and Qarah-Qom regions as highly drought-susceptible and the significant influence of NAO on 66% of stations, this study recommends: 1) Prioritizing drought mitigation investments (e.g., water-efficient agriculture, managed aquifer recharge) in the vulnerable Eastern Border and Qarah-Qom regions. 2) Implementing region-specific NAO-based early warning systems for proactive water allocation. 3) Developing adaptive water resource management plans tailored to decadal drought severity patterns. These targeted strategies enhance resilience to climate-driven droughts in Iran.

Acknowledgments:
The authors confirm that this article was not under any financial support.

Author Contributions:
Javad Momeni Damaneh: Modeling, performing software analysis, Methodology, conceptualization, validation, and writing-editing the article.
Seyed Mohammad Tajbakhsh Fakhrabadi: Methodology, conceptualization, validation, and writing-editing the article.
Ehsan Tamassoki: Modeling, performing software analysis, and writing-editing the article.

Conflicts of interest
The authors of this article declared no conflict of interest regarding the authorship or publication of this article.

Data availability statement:
The datasets are available upon a reasonable request to the corresponding author.

References
Abdelkader, M., & Yerdelen, C. (2022). Hydrological drought variability and its teleconnections with climate indices. Journal of hydrology, 605, 127290.doi: 10.1016/j.jhydrol.2021.127290

Abdelkader, M., & Yerdelen, C. (2022). Hydrological drought variability and its teleconnections with climate indices. Journal of hydrology, 605,

127290. doi: 10.1016/j.jhydrol.2021.127290

Abhilash, S., Krishnakumar, E. K., Vijaykumar, P., Sahai, A. K., Chakrapani, B., & Gopinath, G. (2019). Changing characteristics of droughts over Kerala, India: inter-annual variability and trend. Asia-Pacific Journal of Atmospheric Sciences, 55(1), 1-17. doi:10.1007/s13143-018-0060-9.

AghaKouchak, A., Mirchi, A., Madani, K., Di Baldassarre, G., Nazemi, A., Alborzi, A., Anjileli, H., Azarderakhsh, M., Chiang, F., Hassanzadeh, E. and Huning, L.S. (2021). Anthropogenic drought: Definition, chal- lenges, and opportunities. Reviews of Geophysics, 59(2). doi: 10.1029/2019rg000683

Apurv, T., Sivapalan, M., & Cai, X. (2017). Understanding the role of climate characteristics in drought propagation. Water Resources Research, 53(11), 9304–9329. doi: 10.1002/2017wr021445

Brasil Neto, R.M., Santos, C.A.G., Nascimento, T.V.M., Silva, R.M., Santos, C.A.C. (2020). Evaluation of the TRMM product for monitoring drought over Paraíba State, northeastern Brazil: a statistical analysis. Remote Sensing, 12(14), 2184. doi: 10.3390/rs12142184

Brasil Neto, R.M., Santos, C.A.G., Silva, J.F.C.B.d.C., Silva, R.M., Santos, C.A.C., Mishra, M. (2021). Evaluation of the TRMM product for monitoring drought over Paraíba State, northeastern Brazil: a trend analysis. Scientific Reports, 11(1), 1097. doi: 10.1038/s41598-020-80026-5

Brasil Neto, R.M., Santos, C.A.G., Silva, R.M., Dos Santos, C.A.C. (2022). Evaluation of TRMM satellite dataset for monitoring meteorological drought in northeastern Brazil. Hydrological Sciences Journal, 67(14), 2100-2120. doi:10.1080/02626667.2022.2130333

Burn, D. H., & Whitfield, P. H. (2016). Changes in floods and flood regimes in Canada. Canadian Water Resources Journal/Revue canadienne des ressources hydriques, 41(1-2), 139-150. doi:10.1080/07011784.2015.1026844

Cai, W., Borlace, S., Lengaigne, M., Van Rensch, P., Collins, M., Vecchi, G., Timmermann, A., Santoso, A., McPhaden, M.J., Wu, L. and England, M.H. (2014). Increasing frequency of extreme El Niño events due to greenhouse warming. Nature climate change, 4(2), 111-116. doi: 10.1038/nclimate2100

Caloiero, T., & Veltri, S. (2019). Drought assessment in the Sardinia Region (Italy) during 1922–2011 using the standardized precipitation index. Pure and Applied Geophysics, 176(2), 925-935. doi: 10.1007/s00024-018-2008-5

Caloiero, T., Coscarelli, R., Ferrari, E., Mancini, M. (2011). Precipitation changes in Southern Italy linked to global scale oscillation indexes. Natural Hazards and Earth System Sciences, 11(6), 1683-1694. doi.org/10.5194/nhess-11-1683-2011

Chen, L., Brun, P., Buri, P., Fatichi, S., Gessler, A., McCarthy, M. J., Pellicciotti, F., Stocker, B. & Karger, D. N. (2025). Global increase in the occurrence and impact of multiyear droughts. Science, 387(6731), 278-284. doi:10.1126/science.ado4245

Collins, M., An, S.I., Cai, W., Ganachaud, A., Guilyardi, E., Jin, F.F., Jochum, M., Lengaigne, M., Power, S., Timmermann, A. and Vecchi, G. (2010). The impact of global warming on the tropical Pacific Ocean and El Niño. Nature Geoscience, 3(6), 391-397. doi:10.1038/ngeo868

Dai, A. (2011). Drought under global warming: a review. Wiley Interdisciplinary Reviews: Climate Change, 2(1), 45-65. doi:10.1002/wcc.81

Dai, A., Zhao, T., & Chen, J. (2018). Climate change and drought: a precipitation and evaporation perspective. Current Climate Change Reports, 4, 301-312. doi:10.1007/s40641-018-0101-6

Du, J., Kimball, J.S., Sheffield, J., Velicogna, I., Zhao, M., Pan, M., Fisher, C.K., Beck, H.E., Watts, J.D. and Wood, E.F. (2021). Synergistic satellite assessment of global vegetation health in relation to ENSO-induced droughts and pluvials. Journal of Geophysical Research: Biogeosciences, 126(5), e2020JG006006. doi:10.1029/2020JG006006

Dutta, D., & Herath, S. (2004, July). Trend of floods in Asia and flood risk management with integrated river basin approach. In Proceedings of the 2nd international conference of Asia-Pacific hydrology and water resources Association, Singapore (Vol. 1, pp. 55-63).

Ganguli, P., Majhi, A., & Kumar, R. (2022). Observational evidence for multivariate drought hazard amplifications across disparate climate regimes. Earth's Future, 10(9), e2022EF002809. doi: 10.1029/2022EF002809

Ghazaryan, G., König, S., Rezaei, E. E., Siebert, S., & Dubovyk, O. (2020). Analysis of drought impact on croplands from global to regional scale: a remote sensing approach. Remote Sensing, 12(24), 4030. doi: 10.3390/rs12244030

Grimm, A. M., & Tedeschi, R. G. (2009). ENSO and extreme rainfall events in South America. Journal of Climate, 22(7), 1589-1609. doi:10.1175/2008JCLI2429.1

Herrera-Estrada, J. E., Satoh, Y., & Sheffield, J. (2017). Spatiotemporal dynamics of global drought. Geophysical Research Letters, 44(5), 2254-2263. doi:10.1002/2016GL071768

Hoerling, M., Eischeid, J., Perlwitz, J., Quan, X., Zhang, T., Pegion, P. (2012). On the increased frequency of Mediterranean drought. Journal of

climate, 25(6), 2146-2161.

Holgate, C.M., Falster, G.M., Gillett, Z.E., Goswami, P., Grant, M.O., Hobeichi, S., Hoffmann, D., Jiang, X., Jin, C., Lu, X. and Mu, M. (2025). Physical mechanisms of meteorological drought development, intensification and termination: an Australian review. Communications earth & environment, 6(1), 220. doi: 10.1038/s43247-025-02179-3

Hosseinzadehtalaei, P., Van Schaeybroeck, B., Termonia, P., & Tabari, H. (2023). Identical hierarchy of physical drought types for climate change signals and uncertainty. Weather and Climate Extremes, 41, 100573. doi: 10.1016/j.wace.2023.100573

Huning, L., & AghaKouchak, A. (2020). Global snow drought hot spots and characteristics. Proceedings of the National Academy of Sciences, 117(33), 19753–19759. Doi: 10.1073/pnas.1915921117

Karamouz, M., Araghinejad, S., & Dezfuli, A. K. (2004). Climate regionalizing for the assessment of ENSO, NAO and SST effect on regional meteorological drought: Application of fuzzy clustering. In Critical Transitions in Water and Environmental Resources Management (pp. 1-10). doi:10.1061/40737

Kelley, C., Ting, M., Seager, R., Kushnir, Y. (2012). Mediterranean precipitation climatology, seasonal cycle, and trend as simulated by CMIP5. Geophysical Research Letters, 39(21).

Kenawy, A. E., Al-Awadhi, T., Abdullah, M., Ostermann, F. O., & Abulibdeh, A. (2025). A Multidecadal Assessment of Drought Intensification in the Middle East and North Africa: The Role of Global Warming and Rainfall Deficit. Earth Systems and Environment, 1-20. doi: 10.1007/s41748-025-00576-4

Li, Z., Huang, S., Zhou, S., Leng, G., Liu, D., Huang, Q., et al. (2021). Clarifying the propagation dynamics from meteorological to hydrological drought induced by climate change and direct human activities. Journal of Hydrometeorology, 22(9), 2359–2378. doi:10.1175/ jhm-d-21-0033.1

Limones, N., Molina, J. V., & Paneque, P. (2022). Spatiotemporal characterization of meteorological drought: a global approach using the Drought Exceedance Probability Index (DEPI). Climate Research, 88, 137-154. doi: 10.3354/cr01703

Lin, J., Qian, T., & Schubert, S. (2022). Droughts and Mega-droughts. Atmosphere-Ocean, 60(3-4), 245-306. doi: 10.1080/07055900.2022.2086848

Lloyd-Hughes, B., & Saunders, M. A. (2002). A drought climatology for Europe. International journal of climatology, 22(13), 1571-1592.

Masih, I., Maskey, S., Mussá, F. E. F., & Trambauer, P. (2014). A review of droughts on the African continent: a geospatial and long-term perspective. Hydrology and earth system sciences, 18(9), 3635-3649. doi:10.5194/hess-18-3635-2014

Mathbout, S., Lopez-Bustins, J. A., Royé, D., & Martin-Vide, J. (2021). Mediterranean-scale drought: Regional datasets for exceptional meteorological drought events during 1975–2019. Atmosphere, 12(8), 941.

Mirza, M. M. Q. (2003). Climate change and extreme weather events: can developing countries adapt? Climate policy, 3(3), 233-248. doi:10.3763/cpol.2003.0330

Momeny damaneh J, Tajbakhsh fakhrabadi M, Chezgy J, Tamasoki E. (2024). Spatial correlation of extreme temperatures and vegetation changes in the watersheds of Iran. Iranian Journal of Rainwater Catchment Systems, 12(2), 39-58. http://jircsa.ir/article-1-532-en.html

Nieves, A., Contreras, J., Pacheco, J., Urgilés, J., García, F., & Avilés, A. (2022). Assessment of drought time-frequency relationships with local atmospheric-land conditions and large-scale climatic factors in a tropical Andean basin. Remote Sensing Applications: Society and Environment, 26, 100760. doi: 10.1016/j.rsase.2022.100760

Nikraftar, Z., Mostafaie, A., Sadegh, M., Afkueieh, J.H. and Pradhan, B. (2021). Multi-type assessment of global droughts and teleconnections. Weather and Climate Extremes, 34, 100402. doi: 10.1016/j.wace.2021.100402

Niu, Q., She, D., Xia, J., Zhang, Q., Zhang, Y., & Wang, T. (2025). Uncertainty analysis of global meteorological drought in CMIP6 projections. Climatic Change, 178(4), 1-23. doi: 10.1007/s10584-025-03919-2

Paredes-Trejo, F., Olivares, B. O., Movil-Fuentes, Y., Arevalo-Groening, J., & Gil, A. (2023). Assessing the spatiotemporal patterns and impacts of droughts in the Orinoco River basin using earth observations data and surface observations. Hydrology, 10(10), 195. doi:10.3390/hydrology10100195

Rasmusson, E. M. (2019). Global prospects for the prediction of drought: A meteorological perspective. In Planning for Drought (pp. 31-43). Routledge. doi: 10.4324/9780429301735-3

Rodríguez., JV, Molina., PP, Salgado. (2022). Spatiotemporal characterization of meteorological drought: a global approach using the Drought Exceedance Probablity Index. Climate Research, 88:137-154. doi: 10.3354/cr01703

Santos, C.A.G., Brasil Neto, R.M., Nascimento, T.V.M., Silva, R.M., Mishra, M., Frade, T. G.(2020). Geospatial drought severity analysis

based on PERSIANN-CDR-estimated rainfall data for Odisha state in India (1983–2018). Science of the Total Environment, 750, 141258. doi: 10.1016/j.scitotenv.2020.141258.

Sattari, M.T., Falsafian, K., Irvem, A., Qasem, S.N. (2020). Potential of kernel and tree-based machine-learning models for estimating missing data of rainfall. Engineering Applications of Computational Fluid Mechanics, 14(1), 1078-1094. doi: 10.1080/19942060.2020.1803971

Schubert, S.D., Stewart, R.E., Wang, H., Barlow, M., Berbery, E.H., Cai, W., Hoerling, M.P., Kanikicharla, K.K., Koster, R.D., Lyon, B. and Mariotti, A. (2016). Global meteorological drought: a synthesis of current understanding with a focus on SST drivers of precipitation deficits. Journal of Climate, 29(11), 3989-4019. doi:10.1175/JCLI-D-15-0452.1.

Schubert, S.D., Stewart, R.E., Wang, H., Barlow, M., Berbery, E.H., Cai, W., Hoerling, M.P., Kanikicharla, K.K., Koster, R.D., Lyon, B. and Mariotti, A. (2016). Global meteorological drought: a synthesis of current understanding with a focus on SST drivers of precipitation deficits. Journal of Climate, 29(11), 3989-4019. doi:10.1175/JCLI-D-15-0452.1

Spinoni, J., Naumann, G.Vogt, J.V. Barbosa, P. (2015). The biggest drought events in Europe from 1950 to 2012. Journal of Hydrology: Regional Studies, 3, 509-524. doi: 10.1016/j.ejrh.2015.01.001

Tabari, H., Hosseinzadehtalaei, P., Thiery, W., Willems, P. (2021). Amplified drought and flood risk under future socioeconomic and climatic change. Earth's Future 9 (10), e2021EF002295.

Tajbakhsh Fakhrabadi, S. M. and Momeny, J. (2023). Analysis and Zonation of Drought and the Impact of SOI and NAO on the Six Watersheds of Iran. Water and Soil Science, 33(1), 161-179. doi: 10.22034/ws.2021.44983.2407

Taylor, C.M., Lambin, E.F., Stephenne, N., Harding, R.J., Essery, R.L., 2002. The influence of land use change on climate in the Sahel. Journal of Climate, 15(24), 3615-3629.

Tijdeman, E., Barker, L. J., Svoboda, M. D., & Stahl, K. (2018). Natural and human influences on the link between meteorological and hydrological drought indices for a large set of catchments in the contiguous United States. Water Resources Research, 54(9), 6005–6023. doi:10.1029/2017wr022412

Tokinaga, H., Xie, S. P., Deser, C., Kosaka, Y., & Okumura, Y. M. (2012). Slowdown of the Walker circulation driven by tropical Indo-Pacific warming. Nature, 491(7424), 439-443. doi:10.1038/nature11576.

Van Loon, A. F. (2015). Hydrological drought explained. Wiley Interdisciplinary Reviews: Water, 2(4), 359-392., doi:10.1002/wat2.1085.

Van Loon, A. F., & Van Lanen, H. A. J. (2012). A process-based typology of hydrological drought. Hydrology and Earth System Sciences, 16(7), 1915–1946. doi: 10.5194/hess-16-1915-2012

Van Loon, A. F., Gleeson, T., Clark, J., Van Dijk, A. I. J. M., Stahl, K., Hannaford, J., et al. (2016). Drought in the anthropocene. Nature Geoscience, 9(2), 89–91. doi:10.1038/ngeo2646

Van Loon, A. F., Tijdeman, E., Wanders, N., Van Lanen, H. A. J., Teuling, A. J., & Uijlenhoet, R. (2014). How climate seasonality modifies drought duration and deficit. Journal of Geophysical Research: Atmospheres, 119(8), 4640–4656. doi: 10.1002/2013jd020383

Vicente-Serrano, S. M., Beguería, S., Lorenzo-Lacruz, J., Camarero, J. J., López-Moreno, J. I., Azorin-Molina, C., et al. (2012). Performance of drought indices for ecological, agricultural, and hydrological applications. Earth Interactions, 16(10), 1–27. doi: 10.1175/2012ei000434.1

Vicente-Serrano, S.M., López-Moreno, J.I., Lorenzo-Lacruz, J., El Kenawy, A., Azorin-Molina, C.,Morán-Tejeda, E., Pasho, E., Zabalza, J., Begueria, S., Angulo-Martinez, M. (2011). The NAO impact on droughts in the Mediterranean region. Hydrological, socioeconomic and ecological impacts of the north Atlantic oscillation in the mediterranean region, 23-40.

Vieira, M.J. and Stadnyk, T.A. (2023). Leveraging global climate models to assess multi-year hydrologic drought. npj Climate and Atmospheric Science, 6(1), 179. doi: 10.1038/s41612-023-00496-y

VijayaVenkataRaman, S., Iniyan, S., & Goic, R. (2012). A review of climate change, mitigation and adaptation. Renewable and Sustainable Energy Reviews, 16(1), 878-897. doi: 10.1016/j.rser.2011.09.009.

Wang, G.C., Zhang, Q., Band, S.S., Dehghani, M., Chau, K.W., Tho, Q.T., Zhu, S., Samadianfard, S., Mosavi, A. (2022). Monthly and seasonal hydrological drought forecasting using multiple extreme learning machine models. Engineering Applications of Computational Fluid Mechanics, 16(1), 1364-1381. doi: 10.1080/19942060.2022.2089732

Wu, G., Chen, J., Kim, J. S., Gu, L., Lee, J. H., & Zhang, L. (2022). Impacts of climate change on global meteorological multi-year droughts using the last millennium simulation as a baseline. Journal of Hydrology, 610, 127937. doi: 10.1016/j.jhydrol.2022.127937

Wu, J., & Dirmeyer, P. A. (2020). Drought demise attribution over conus. Journal of Geophysical esearch: Atmospheres, 125(4), e2019JD031255. doi: 10.1029/2019jd031255

Xu, Y., Yang, Z., Zhang, L., & Zhang, J. (2025). An Evaluation of the Capability of Global Meteorological Datasets to Capture Drought Events in Xinjiang. Land, 14(2), 219. doi:10.3390/land14020219

Yang, R., & Xing, B. (2022). Teleconnections of large-scale climate patterns to regional drought in mid-latitudes: A case study in Xinjiang, China. Atmosphere, 13(2), 230. doi: 10.3390/atmos13020230

Yuce, M. I., Aytek, A., Esit, M., Deger, I. H., Yasa, I., Simsek, A., & Ugur, F. (2025). Investigation of the meteorological and hydrological drought characteristics in yeşilirmak basin, Türkiye. Theoretical and Applied Climatology, 156(4), 1-16. doi: 10.1007/s00704-025-05437-8

Zeng, J., Li, J., Lu, X., Wei, Z., Shangguan, W., Zhang, S., Dai, Y. and Zhang, S. (2022). Assessment of global meteorological, hydrological and agricultural drought under future warming based on CMIP6. Atmospheric and Oceanic Science Letters, 15(1), 100143. doi: 10.1016/j.aosl.2021.100143

Zhao, C., Huang, Y., Li, Z., Chen, M. (2018). Drought monitoring of Southwestern China using insufficient GRACE data for the long-term mean reference frame under global change. Journal of Climate. 31, 6897–6911. doi: 10.1175/JCLI-D-17-0869.1

Zhao, T., Dai, A. (2022). CMIP6 model-projected hydroclimatic and drought changes and their causes in the twenty-first century. Journal of Climate. 35 (3), 897–921. doi: 10.1175/JCLI-D-21-0442.1

Zhu, Z., Duan, W., Zou, S., Zeng, Z., Chen, Y., Feng, M., Qin, J. and Liu, Y. (2024). Spatiotemporal characteristics of meteorological drought events in 34 major global river basins during 1901–2021. Science of The Total Environment, 921, 170913. doi: 10.1016/j.scitotenv.2024.170913